Harada, N., Miwa, G. T., Walsh, J. S., & Lu, A. Y. H. (1984) *J. Biol. Chem. 259* 3005–3010.
Huckin, S. N., & Weiler, L. (1974) *J. Am. Chem. Soc. 96*, 1082–1087.
Jones, J. P., Korzekwa, K. R., Rettie, A. E., & Trager, W. F. (1986) *J. Am. Chem. Soc. 108*, 7074–7078.
Karp, F., & Croteau, R. (1982) *Arch. Biochem. Biophys. 216*, 616–624.
Kluger, R., & Brandl, M. (1986) *J. Org. Chem. 51*, 3964–3968.
Liu, K.-T., & Wu, Y. W. (1986) *Tetrahedron Lett.*, 3623–3626.
McCormick, J. P., & Barton, D. L. (1978) *Tetrahedron 34*, 325–330.
Pascal, R. A., Jr., Baum, M. W., Wagner, C. K., Rodgers, L. R., & Huang, D.-S. (1986) *J. Am. Chem. Soc. 108*, 6477–6482.
Samuelson, A. G., & Carpenter, B. K. (1981) *J. Chem. Soc., Chem. Commun.*, 354–356.
Satterwhite, D. M., Wheeler, C. J., & Croteau, R. (1985) *J. Biol. Chem. 260*, 13901–13908.
Still, W. C., Kahn, M., & Mitra, A. (1978) *J. Org. Chem. 43*, 2923–2925.
Sunko, D. E., Szele, I., & Hehre, W. J. (1977) *J. Am. Chem. Soc. 99*, 5000–5005.
Weiler, L. (1970) *J. Am. Chem. Soc. 92*, 6702–6704.
Wheeler, C. J., & Croteau, R. (1986a) *Arch. Biochem. Biophys. 246*, 733–742.
Wheeler, C. J., & Croteau, R. (1986b) *Arch. Biochem. Biophys. 248*, 429–434.
Wheeler, C. J., & Croteau, R. (1987) *J. Biol. Chem. 262*, 8213–8219.
Winkle, M. B., Lansinger, J. M., & Ronald, R. C. (1980) *J. Chem. Soc., Chem. Commun.*, 87–88.

Spontaneous Fusion of Phosphatidylcholine Small Unilamellar Vesicles in the Fluid Phase†

Barry R. Lentz,* Tamra J. Carpenter,‡ and Dennis R. Alford§
Department of Biochemistry and Nutrition, The University of North Carolina at Chapel Hill, Chapel Hill, North Carolina 27514

Received September 18, 1986; Revised Manuscript Received January 20, 1987

ABSTRACT: Using a high-sensitivity differential scanning microcalorimeter capable of performing cooling scans, we have examined the phase behavior of small unilamellar vesicles (SUV) as a function of time of storage above their order–disorder phase transition. Vesicles composed of dipalmitoylphosphatidylcholine (DPPC) and dimyristoylphosphatidylcholine (DMPC) were examined. Cooling scans on fresh (5–7-h postsonication) samples revealed broad, relatively simple heat capacity peaks (peak temperatures: 19.9 °C for DMPC, 37.8 °C for DPPC) free of high-temperature spikes or shoulders. Subsequent heating scans displayed a sharp peak characteristic of previously described fusion products formed below the phase transition. SUV samples stored for 1 or more days above their phase transition displayed a moderately broad, high-temperature shoulder (23.8 °C for DMPC and 40.2 °C for DPPC) in the cooling profile. For DMPC, the enthalpy associated with this peak increased in a first-order fashion with time. Hydrolysis products were not detected until 12–20 days of storage. Both the rate and extent of shoulder appearance increased with temperature (k = 0.0017 h^{-1}, fraction of total enthalpy = 0.1 at 36 °C; k = 0.0037 h^{-1}, fraction = 0.2 at 42 °C). Freeze–fracture electron micrographs confirmed that an intermediate-sized vesicle population (diameters 400–500 Å) appeared in SUV samples stored above their phase transition. Also, the trapped volume of DMPC SUV increased from 0.26 μL/μmol after 17 h of storage to 0.54 μL/μmol after storage for 16 days at 36 °C. We ruled out the possibility that esterolytic hydrolysis products might be responsible for inducing membrane fusion by performing experiments with ditetradecylphosphorylcholine, an ether lipid analogue of DMPC. Comparable results were obtained (k = 0.0047 h^{-1}, fraction = 0.25 at 41.5 °C). Our results demonstrate that at least a subpopulation of a normal SUV preparation is thermodynamically unstable even above the SUV phase transition.

Sonicated small unilamellar vesicles (SUV)[1] and large multilamellar or large unilamellar vesicles (LMV or LUV) are popular systems for modeling the properties of the phospholipid bilayer portions of biological membranes. However, use of SUV has been limited to modeling the effects of local bilayer curvature on biomembrane properties (Sackmann et al., 1984; Gruner, 1985). This is because SUV experience molecular packing constraints resulting from their high curvature (Sheetz & Chan, 1972; Huang & Mason, 1978). The packing inhomogeneities caused by high curvature are believed to account for the unique physical properties of SUV. Among these are the asymmetric distribution of certain phospholipid species between the inner and outer leaflets of the bilayer

† Supported by USPHS Grant GM 32707.
* Address correspondence to this author.
‡ Present address: Operations Research Analyst, RCA Staff Center, Princeton, NJ 08540.
§ Present address: Department of Pharmacy and Pharmaceutical Chemistry, School of Pharmacy, University of California at San Francisco, San Francisco, CA 94143.

[1] Abbreviations: SUV, small unilamellar vesicles(s); LMV, large multilamellar vesicle(s); LUV, large unilamellar vesicle(s); DPPC, 1,2-dipalmitoyl-3-*sn*-phosphatidylcholine; DMPC, 1,2-dimyristoyl-3-*sn*-phosphatidylcholine; DTPC, 1,2-ditetradecyl-3-*sn*-phosphorylcholine; HPLC, high-performance liquid chromatography.

0006-2960/87/0426-5389$01.50/0

(Thompson et al., 1974), the observed instability of SUV below their order–disorder phase transition (Suurkuusk et al., 1976), and the lower cooperativity of the phase transition in SUV as opposed to LMV (Sheetz & Chan, 1972; Suurkuusk et al., 1976) or LUV (Parente & Lentz, 1984). Instability below the phase transition manifests itself in terms of SUV fusion to yield LUV (Wong et al., 1982) or other more complex structures (Larabee, 1979). By contrast, it has generally been reported that SUV are stable when maintained above the order–disorder phase transition (Suurkuusk et al., 1976; Schullery et al., 1980; McConnell & Schullery, 1985), although reports of SUV properties free of any indication of contamination by larger species are rare.

The wide use of SUV as model membranes clearly makes the issue of vesicle stability one of great practical importance. Beyond this, however, this issue has fundamental significance in terms of defining the most stable aggregation state of phospholipids suspended in an aqueous environment. Because of the molecular packing strain accompanying high bilayer curvature, one might expect that SUV represent a thermodynamically unstable state that is formed due to high energy input during sonication. The present study addresses this issue by examining the time evolution of the unique phase behavior of SUV preparations stored at temperatures above the phase transition.

The phase behavior of SUV preparations has been difficult to establish by calorimetry due mainly to the presence of large vesicle contaminants. Equilibration of an SUV preparation at low temperature before beginning a calorimetric scan inevitably results in formation of fusion products, which obscure the phase behavior of the SUV [e.g., see Suurkuusk et al. (1976) and Dufour et al. (1981)]. We report here the phase behavior of SUV preparations maintained for differing lengths of time exclusively above their phase transition temperature. This has been possible because unlike most high-sensitivity differential scanning calorimeters ours is capable of performing cooling scans with sensitivity and reproducibility comparable to those attainable in heating scans. Our calorimetric results, along with freeze–fracture electron micrographs and trapped volume determinations on the stored samples, demonstrate that SUV changed slowly to a mixture of small and intermediate-size (400–500-Å diameters) unilamellar vesicles, even when stored in the fluid state. The conversion to intermediate vesicles was incomplete, with only the most highly curved vesicles being converted to larger ones. The fraction converted to larger vesicles increased with temperature. We have interpreted these results as demonstrating fusion of highly curved vesicles even above their order to disorder phase transition.

Materials and Methods

Materials. Chloroform solutions of recrystallized (Lentz et al., 1976) 1,2-dimyristoyl-3-*sn*-phosphatidylcholine (DMPC) and 1,2-dipalmitoyl-3-*sn*-phosphatidylcholine (DPPC) were obtained from Avanti Biochemicals (Birmingham, AL) and determined to contain less than 1 mol % polar lipid impurity by thin-layer chromatography (Lentz et al., 1976). 1,2-Ditetradecyl-3-*sn*-phosphorylcholine (DTPC) (the ether lipid analogue of DMPC) was obtained from Berchtold Biochemiches Labor (Bern, Switzerland), stocked in HPLC-grade chloroform (Fisher Chemical Co.), and used with no further purification after its purity was checked by thin-layer chromatography (Lentz et al., 1976). Aqueous suspensions of phospholipids were prepared by using ultrapure KCl (50 mM) (Heico, Inc., Delaware Water Gap, PA) and water that was doubly distilled from glass. All other reagents were of the best quality available.

Model Membranes. Small unilamellar vesicles were prepared by direct probe sonication using a Heat Systems W350 Sonifier equipped with a titanium probe tip (Suurkuusk et al., 1976). DMPC or DPPC small vesicles were fractionated from larger ones by using high-speed centrifugation (Barenholz et al., 1977). DTPC vesicles were less dense than the aqueous medium and floated when subjected to high-speed centrifugation. For this reason, DTPC vesicles required fractionation by size-exclusion chromatography (Huang, 1969) on a Sepharose CL-4B (Pharmacia Fine Chemicals, Upsula, Sweden) column (62 × 2.5 cm) equilibrated and run at 38 °C. Unless otherwise stated, vesicle samples were maintained rigorously above their phase transition temperature at all times during and following sonication. Concentrations of phospholipid suspensions were determined by inorganic phosphorus analysis (Chen et al., 1956) to a precision of ±1.5% for homogeneous suspensions and ±2.5% for less homogeneous suspensions.

In order to check for hydrolytic degradation of phospholipid during storage of SUV samples, these were routinely extracted with HPLC-grade $HCCl_3/H_3COH$ (Bligh & Dyer, 1959). The extract was dried with anhydrous sodium metabisulfite and analyzed by silicic acid thin-layer chromatography (Lentz et al., 1976). With heavy loading of the thin-layer plate (0.5–1 μmol) and staining by I_2 vapors, this method was capable of detecting 2–4 mol % contamination by lysophosphatidylcholine, the hydrolytic breakdown product of phosphatidylcholine.

Calorimetry. Cooling and subsequent heating scans were made on vesicle samples by using a high-sensitivity differential scanning calorimeter constructed for us by Roger Hart (Hart Scientific, Orem, UT). This instrument is an improvement of the basic heat flow design of Suurkuusk et al. (1976), having both increased sensitivity and the ability to cool conveniently as well as to heat. The accuracy of this instrument and of the computational algorithms used to calculate heat capacities has been established by using standards of known phase behavior (B. R. Lentz, K. W. Clubb, D. Massenberg, R. Hart, and T. E. Jensen, unpublished results). More details on the use of this calorimeter are given elsewhere (Parente & Lentz, 1984). Samples, consisting of 5.3–5.7 mg of phospholipid in 1.5 mL of 50 mM KCl, were sealed in stainless-steel (type 316) ampules and scanned at rates of ±15 °C/h. Vesicle samples were maintained at all times above the phase transition until a scan was begun. This was accomplished while loading the calorimeter ampules by inserting the ampule in a small heating block from which it was removed only momentarily for weighing.

Electron Microscopy. Samples for freeze–fracture were preincubated for 5–10 min at the quenching temperature. A propane jet freezing device was used to very rapidly freeze the samples, which were sandwiched between two thin copper sheets (Lentz et al., 1981). After being fractured in a Balzer's BA360M freeze–etching device at −110 °C and 10^{-6} torr, samples were shadowed with Pt (10 Å) and carbon (50 Å) at an angle of 45°. A JEOL 100 CX microscope operated at 80 kV was used to view freeze–fractured replicas. Mass-weighted vesicle size distributions were calculated as described by Parente and Lentz (1984).

Trapped Volume. The size of internal vesicle compartments was determined by measuring the fluorescence of trapped 6-carboxyfluorescein as described by Parente and Lentz (1984), with the following modifications. Chromatography of the vesicles was on a Sephadex G-75 column at 37 °C. Vesicles were disrupted with 80 mM dodecyl octaoxyethylene glycol monoether to free entrapped 6-carboxyfluorescein before its fluorescence was recorded. Standard curves of carboxy-

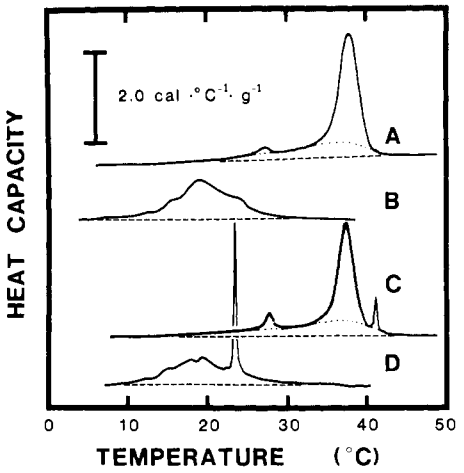

FIGURE 1: Temperature dependence of the specific heat capacity of freshly prepared SUV. Data are presented for SUV prepared from DPPC (A and C) and DMPC (B and D) studied in both cooling (A and B) and subsequent heating (C and D) scans made at ±15 °C/h. Samples were maintained at high temperature (49–53 °C for DPPC; 36–42 °C for DMPC) for 5–7 h following sonication (including fractionation by ultracentrifugation and equilibration in the calorimeter) and before beginning the cooling scan.

fluorescein concentration vs. fluorescence were made by diluting carboxyfluorescein into appropriate detergent/buffer solutions. Carboxyfluorescein fluorescence was monitored with an SLM 4800 spectrofluorometer, with the excitation wavelength set at 490 nm and emission at 530 nm. Phospholipid concentration in these samples was determined by scintillation counting of 1,2-di[1-^{14}C]myristoyl-3-*sn*-phosphatidylcholine (Amersham lot 2100-0786), with which the stock solution of lipid was labeled prior to sonication.

Results

Phase Behavior of Fresh DPPC and DMPC SUV. The phase behavior of both DPPC and DMPC SUV rigorously maintained above their phase transitions prior to scanning was recorded in cooling scans in our differential scanning calorimeter. The results are presented in Figure 1A,B. The cooling scans showed only very broad transitions, with peaks at 19.9 and 37.8 °C for DMPC and DPPC, respectively. Note that for both lipids the heat capacity did not return to the base-line value until well below the main peak. This behavior resulted in an ambiguity as to the limits to use in integrating the heat capacity peaks to obtain the transition enthalpy. This ambiguity was greatest for the DPPC scans, since these contained a relatively sharp main transition peak. For this reason, the DPPC peak was integrated in two ways: first, between wide limits determined by the regions of flat base line (dashed line in Figure 1A); second, according to a curved base line that defined separately both the main transition and the minor, low-temperature peak at 27.4 °C (dotted lines in Figure 1A). The enthalpies obtained from the cooling scan in Figure 1A by these two methods were 9.61 kcal/mol (total, 13–42.5 °C), 6.49 kcal/mol (main peak, 29–42.5 °C), 0.28 kcal/mol (minor, low-temperature peak, 26–29 °C), and 2.83 kcal/mol (residual broad contribution above the dashed base line but below the main and minor peaks as defined by the dotted line, 13–42.5 °C). The DMPC SUV enthalpy was determined to be 5.16 kcal/mol (7–32 °C integration limits).

Heating scans were performed on these same SUV samples immediately following the cooling scans (total time below the phase transition: 270 min, DPPC; 140 min, DMPC). The resulting heat capacity profiles are presented in Figure 1C,D. Both profiles, but especially the DMPC one, displayed a sharp peak (peak temperatures 41.3 and 23.6 °C for DPPC and DMPC, respectively) at temperatures substantially above the broad SUV peaks. These peaks correspond exactly in their maximum temperature to those reported for LMV or LUV composed of these lipids (Parente & Lentz, 1984) and presumably result from fusion products that form rapidly below the SUV phase transition (Suurkuusk et al., 1976). The fusion products resulting from long-term storage of DPPC SUV have been shown to be LUV of 700-Å diameter (Wong et al., 1982), while the products of long-term DMPC SUV storage were more complex (Parente & Lentz, 1984).

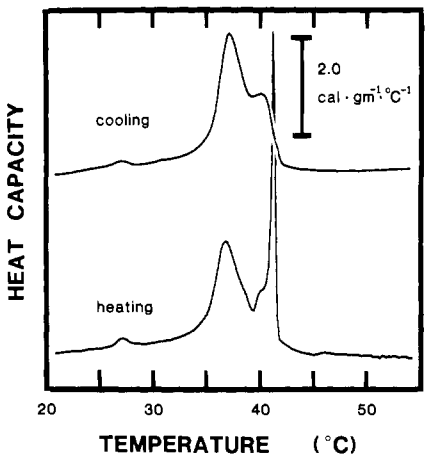

FIGURE 2: Temperature dependence of the specific heat capacity of DPPC SUV stored for 149 h at 49 °C before being equilibrated in the calorimeter at 56 °C for 2 h prior to starting the initial cooling and subsequent heating scans.

Phase Behavior of Stored DPPC and DMPC SUV. In this section, we report the phase behavior of vesicles that were carefully maintained *above* their phase transitions for periods of up to 2 weeks. The effects of vesicle storage *below* the phase transition have been extensively documented (Suurkuusk et al., 1976; Schullery et al., 1980; Wong et al., 1982; Parente & Lentz, 1984; Lichtenberg et al., 1984).

Figure 2 contains heat capacity profiles of DPPC SUV stored for 6 days at 49 °C. Note that the initial cooling profile contained a broad, high-temperature shoulder (peak at 40.2 °C) not present in the profile obtained with fresh vesicles (Figure 1A). The subsequent heating scan on the same sample showed both this broad shoulder and a new, sharp peak at 41.2 °C (Figure 2). Again, the sharp peak probably reflects the formation of LUV below the phase transition (Wong et al., 1982). By contrast, the position and breadth of the shoulder at 40.2 °C suggest the presence in the warm-stored sample of vesicles intermediate in size between SUV and LUV (contrast Figures 1A, 2B, and 2C). This interpretation is consistent with a report on the phase behavior of intermediate-sized vesicles (Lichtenberg et al., 1981). Samples examined after 12 and 20 days of storage showed no appreciable difference in the relative height of the main peak and shoulder, although the main transition width in cooling scans was somewhat broader than in the scan shown in Figure 2 (3.8 °C at 20 days vs. 2.7 °C at 6 days).

In order to test for possible phospholipid hydrolysis during the prolonged storage at high temperature, extracted samples were analyzed by thin-layer chromatography after 5, 9, 12, and 20 days of storage. No hydrolysis products were detected until 12 and 20 days of storage, at which times trace quantities of both lysophosphatidylcholine and fatty acids were in evidence. Appearance of these hydrolysis products might explain the broadening of the main SUV peak also observed at these times (see above).

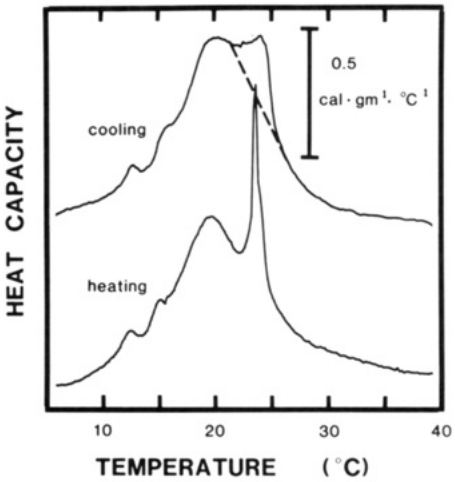

FIGURE 3: Temperature dependence of the specific heat capacity of DMPC SUV stored for 148 h at 36 °C before being equilibrated in the calorimeter at 42 °C for 3 h prior to starting the initial cooling and subsequent heating scans.

Figure 3 documents the phase behavior of a DMPC SUV sample maintained for 6 days at 36 °C. As for the DPPC results in Figure 2, the initial cooling scan revealed a broad shoulder at 23.8 °C which was just barely present in the data obtained with a fresh sample (Figure 1B). The appearance of this peak is presumed to reflect the formation of intermediate-sized vesicles, as in the case of DPPC SUV. In the subsequent heating scan, this broad shoulder was dwarfed by a sharp peak at 23.7 °C (Figure 3). The slight broadening at the base of this sharp peak indicated a small remaining contribution from the broad shoulder. Nonetheless, the substantial disappearance of the broad shoulder in the heating scan indicates that DMPC SUV behaved somewhat differently from DPPC SUV, in which the broad shoulder persisted in heating scans (see Figure 2). This might mean that DMPC high-temperature, intermediate-sized vesicles were unstable and rapidly converted to more stable, larger vesicles below the phase transition.

Extraction and thin-layer chromatographic analysis of DMPC SUV preparations revealed no evidence of hydrolytic degradation after 9 days of storage at 36 °C but did show trace quantities of lysophosphatidylcholine and fatty acid by 15 days of storage, as with DPPC samples.

Freeze–Fracture Electron Microscopy. Electron micrographs of freeze–fracture replicas obtained under several conditions of storage are presented in Figure 4. Except in the case of fresh SUV preparations, convex and concave fracture faces, as well as evidence of some etching, were seen in most replicas, demonstrating that the observed structures correspond to vesicles. SUV appeared mainly as convex faces, sometimes with a slight depression or "dimple", in freeze–fracture replicas (see Figure 7A). This may be because the concave fracture faces of such small structures are expected to be only about 150 Å in diameter before shadowing. Because of these small dimensions, uncertainties in the platinum layer thickness as well as a small degree of etching could give to a concave fracture face the dimpled appearance of some of the structures seen in Figure 4A. We have observed similar images with replicas prepared from DPPC- or 1,2-dipentadecyl-3-*sn*-phosphatidylglycerol-containing SUV preparations (B. R. Lentz, R. A. Parente, and M. Höchli, unpublished results; Lentz et al., 1985).

The micrographs in Figure 4 demonstrate that a uniform population of DMPC small vesicles (Figure 4A) was transformed to be a more heterogeneous population of both small and intermediate-sized vesicles upon prolonged storage at 36 °C (Figure 4B). This point is quantitated by the histograms presented in Figure 5, which were obtained by measuring vesicles in several micrographs. These histograms show that small vesicles were not transformed to large vesicles by storage above their phase transition but rather to intermediate-sized vesicles of only 400–500-Å diameter. Simple calculations of vesicle surface area demonstrate that the intermediate-sized vesicles found in SUV preparations stored above T_m contain the lipid from only two to four SUV. By contrast, Wong et al. (1982) have estimated that roughly 18 small vesicles must fuse to form the 700-Å vesicles observed in DPPC SUV preparations stored *below* T_m. In agreement with these observations, our freeze–fracture data demonstrate that the product of storage of DMPC SUV preparations below T_m (Figure 4C) is much different from the structures formed above T_m (Figure 4B). These morphological observations are all completely consistent with the implications of our phase behavior data (contrast Figures 2A and 3A with Figures 2B and 3B).

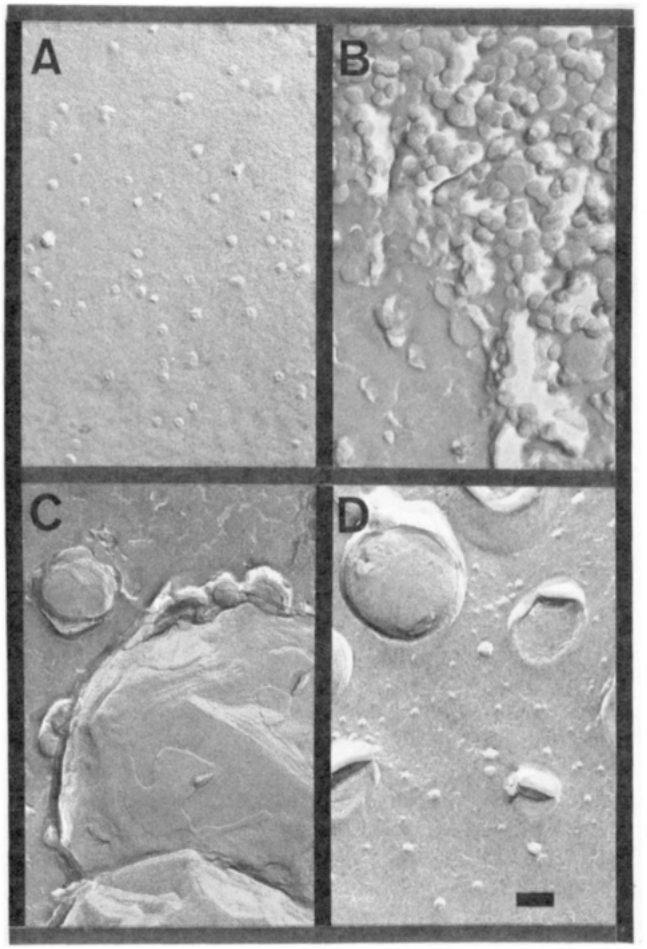

FIGURE 4: Electron micrographs of freeze–fracture replicas of SUV preparations. (A) Fresh DMPC SUV stored for only 5 h at 36 °C and quenched from 36 °C; (B) DMPC SUV stored 19 days at 36 °C (*above* T_m) and quenched from 38 °C; (C) DMPC SUV stored 30 days at 4 °C (*below* T_m) and quenched from 11 °C; (D) DPPC SUV stored 58 days at 50 °C (*above* T_m) and quenched from 58 °C. Magnification for all frames is 50000×; the bar in frame D represents 1000 Å. Shadowing by platinum, in all cases, was from below.

Figure 4D illustrates the results of extensive storage of a DPPC sample above T_m (58 days at 50 °C). The storage products are very different from those formed after 1 or 2 weeks of storage (compare to Figure 4B). The phase behavior of samples stored for 50–60 days (broad peak at ~24 °C for DMPC and at ~41.5 °C for DPPC; data not shown) was also

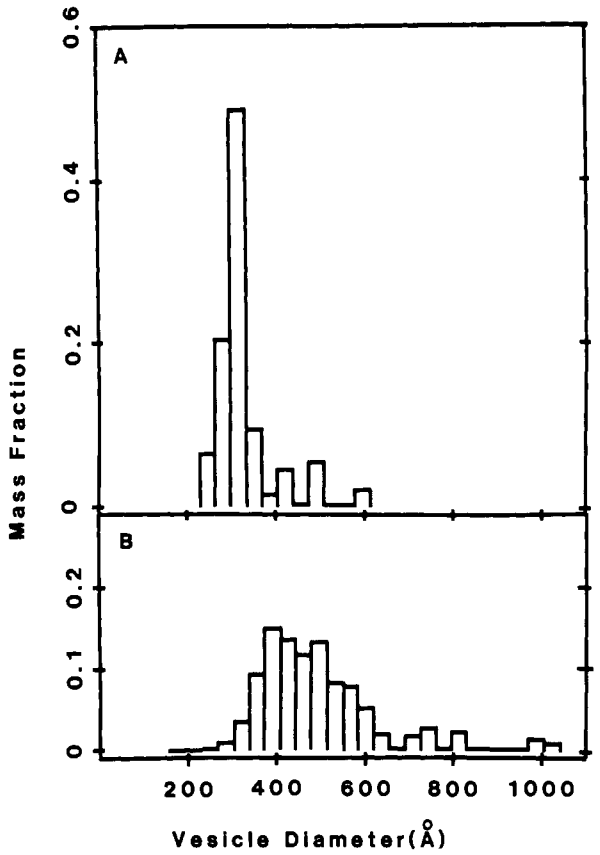

FIGURE 5: Histogram of vesicle mass-weighted diameter distributions existing in DMPC/SUV preparations after 5 (A) or 450 h (B) of storage at 36 °C. Measurements were made at the outer edges of convex fracture faces of 197 and 722 vesicles to obtain the histograms in frames A and B, respectively. The ordinate presents the mass fraction of vesicles whose diameters fall within the 40-Å windows indicated on the abscissa.

not indicative of a mixture of small and intermediate-sized vesicles. Since this behavior was not consistent with that of samples stored for only 1 or 2 weeks, we presume that it is due to the presence of substantial amounts of hydrolysis products, and such extensively stored samples were not considered any further.

Kinetics of Fusion Product Appearance. In order to obtain an estimate of the rate of appearance of intermediate-sized vesicles in DMPC SUV preparations at temperatures above the phase transition, the phase behaviors of samples were monitored calorimetrically as a function of storage time. The enthalpies associated with the small vesicle main transition and with the high-temperature shoulder were calculated as illustrated in Figure 3. These are recorded in Table I. Note that the enthalpy of the main, SUV-associated peak increased slightly with storage time before it began to decrease. This was an unexpected but reproducible phenomenon and may reflect the need to "anneal" small vesicle preparations by storage above their phase transition in order to reach a stable vesicle structure (Lawaczeck et al., 1976).

The kinetics of the fusion process were quantitatively estimated by focusing on the growth of the peak associated with the fusion product (peak α in Table I). The enthalpy of this peak was easily determined and was free of the ambiguities associated with the uncertain base line of the small vesicle peak (see above). The fraction of lipid contributing to this peak (f_L) was calculated as described in the Appendix. This quantity is plotted as a function of storage time at 36 °C (closed squares) and 42 °C (open circles) in Figure 6. From these plots, f_L^* (the limiting value of f_L) was estimated and

Table I: Peak Enthalpies Associated with Stored DMPC SUV Preparations

	storage time (h)	peak α^a ΔH_α (kcal/mol of lipid)	peak β^b ΔH_β (kcal/mol of lipid)
(A) SUV preparation stored at 36 °C	7	0.09	5.07
	67	0.31	5.36
	151	0.47	4.82
	247	0.71	4.66
(B) SUV preparation stored at 42 °C	7	0.08	5.08
	31	0.41	5.68
	367	1.32	4.79

[a] Fusion product peak, T_m = 23.6–24.3 °C (23.8 ± 0.25 °C). [b] SUV peak, T_m = 19.1–20.7 °C (19.9 ± 0.06 °C).

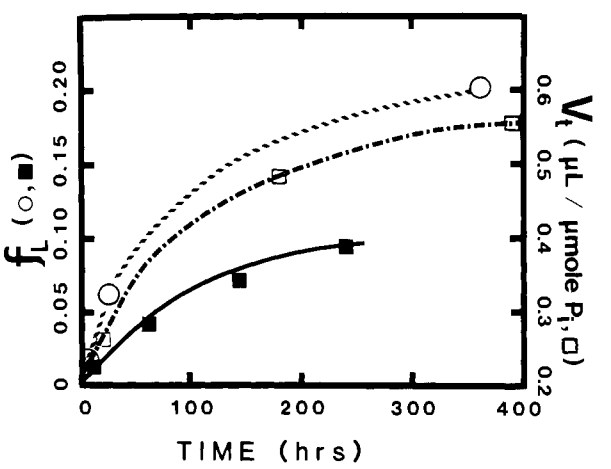

FIGURE 6: Time course for the appearance of intermediate-sized vesicles in DMPC SUV preparations stored above their phase transition. Estimates based on calorimetric data were taken from cooling thermograms of SUV samples (e.g., see Figure 3A; concentrations 4.3–5.7 mM) stored at 36 °C (closed squares) or 42 °C (open circles). The fraction of lipid present as larger vesicles (f_L) was derived as described in the Appendix from the resolved peak enthalpies recorded in Table I. These data were analyzed to yield estimates for the apparent first-order rate constants for large vesicle formation of 0.009 and 0.013 h^{-1} at 36 and 42 °C, respectively (see Appendix). A value of 6.5 kcal/mol (LMV and LUV transition enthalpy; Parente & Lentz, 1984) was assigned to ΔH_L for the purpose of calculating f_L, and values of 0.1 and 0.2 were assigned as equilibrium long-time values of (f_L^*) at 36 and 42 °C, respectively. Evidence for vesicle size increase was also obtained from the increase in trapped volume of a DMPC SUV preparation (concentration 5.4 mM) stored at 37 °C for long times (open squares).

used to transform the data according to the simple, irreversible, pseudo-first-order kinetic model outlined in the Appendix. This analysis gave estimates for the rate constant for conversion of SUV to intermediate-sized vesicles at 36 °C (k = 0.009 ± 0.0004 h^{-1} for f_L^* = 0.1) and 42 °C (k = 0.013 ± 0.001 h^{-1} for f_L^* = 0.2). The error estimates were obtained from the errors in the slope of linear regression lines drawn through the logarithmically transformed data. The numerical values of these kinetic constants depend on our estimates of the limiting (i.e., long-time) values of f_L (f_L^*; see Appendix). With the values of f_L^* indicated above, analysis of the data according to eq 3 of the Appendix yielded values of f_L^0 close to zero, consistent with our observations (see Figure 6). Nonetheless, our inability to measure f_L^* at very long times (due to slow hydrolytic phospholipid breakdown) could lead to systematic errors in the calculated kinetic constants of roughly 10–15%. Despite this uncertainty, it is clear that both the rate and extent of conversion of SUV to larger vesicles increased substantially with temperature.

Trapped Volume Measurements. The trapped volume of DMPC SUV (5.4 mM) was measured by carboxyfluorescein

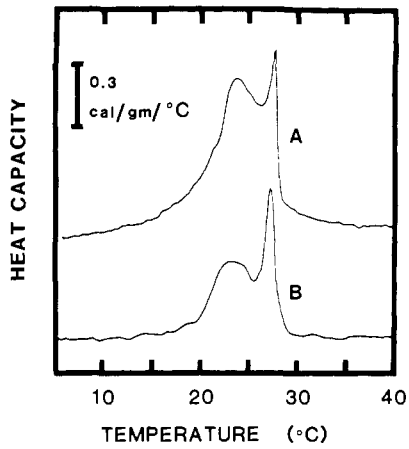

FIGURE 7: Temperature dependence of the specific heat capacity of DTPC SUV stored for 1 (A) or 10 days (B) at 41.5 °C. Cooling scans are shown. Heating scans were similar except that the high-temperature peak was somewhat more narrow.

trapping (see Materials and Methods), and these values are plotted in Figure 6 (open squares) as a function of storage time at 36 °C. Because of the need to soak the vesicles in carboxyfluorescein overnight (Parente & Lentz, 1984), the first determination was made on SUV that had been stored for 17 h. Following this determination, the trapped volume increased with storage time in a fashion very similar to that seen for the increase in f_L (see Figure 6). Extrapolating back to time zero, the trapped volume of "fresh" SUV can be seen to be approximately 0.2 μL/μmol of phosphate, a value consistent with previous reports for fresh SUV (0.17 μL/μmol for egg phosphatidylcholine; Roseman et al., 1978; Parente & Lentz, 1984). The long-time, limiting trapped volume (0.54 μL/μmol of phosphate; see Figure 6) implies a shift in the vesicle population toward vesicles of intermediate size (if we assume f_L^* = 0.1–0.2, the trapped volume is consistent with outer diameters of 450–500 Å), in agreement with our electron microscopic results (Figures 4 and 5).

Phase Behavior and Fusion of DTPC SUV. Although we have not found significant quantities of hydrolysis products in DPPC and DMPC SUV preparations stored above their phase transitions for under 12 days, there does remain the possibility that very small quantities of lysophosphatidylcholine or fatty acid could have escaped detection by our thin-layer chromatographic analysis. Therefore, small amounts of hydrolysis products could have induced the fusion we have observed above the phase transition of SUV preparations. In addition, the small quantities of hydrolysis products that we have detected in DMPC or DPPC SUV preparations *after* 12 days of storage could have enhanced the rate or extent of fusion for samples stored greater than 12 days. To test for these possibilities, we studied the phase behavior of SUV prepared from DTPC. This phospholipid is analogous to DMPC in its structure but has ether linkages from the glycerol backbone to *alkyl* (instead of *acyl*) hydrophobic chains. These ether bonds are considerably more resistant to hydrolytic cleavage than are the ester bonds of DMPC.

The specific heat capacity temperature profiles of DTPC SUV after 1 day (curve A) or 10 days (curve B) of storage at 41.5 °C are presented in Figure 7. Unlike DMPC and DPPC SUV, even fresh (6–8 h of storage) DTPC SUV preparations showed a significant high-temperature shoulder on the specific heat capacity profile (not shown). This could result from the different method of SUV fractionation required for DTPC vs. DMPC or DPPC preparations (size-exclusion chromatography vs. differential sedimentation; see Materials and Methods). As with DMPC and DPPC preparations, however, the enthalpy associated with this shoulder increased with storage time, even above the phase transition, as documented in Table II.

Table II: Peak Enthalpies Associated with DTPC SUV Preparation Stored at 41.5 °C

storage time (h)	peak α^a ΔH_α (kcal/mol of lipid)	peak β^b ΔH_β (kcal/mol of lipid)
6	0.69	2.70
24	0.50	3.00
72	0.65	2.85
240	1.02	2.50
432	1.12	2.58

[a] Fusion product peak, T_m = 27.0–27.5 °C (27.3 ± 0.2 °C). [b] SUV peak, T_m = 22.8–24.0 °C (23.3 ± 0.4 °C).

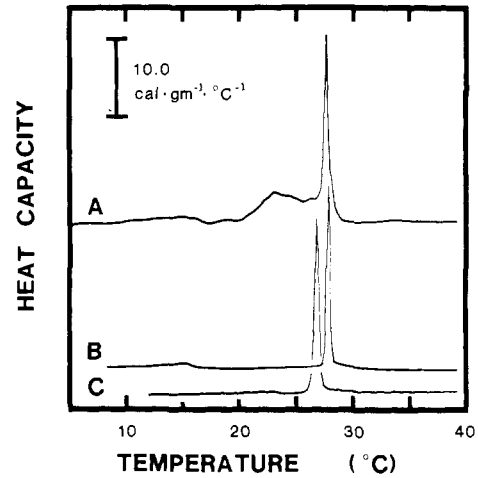

FIGURE 8: Temperature dependence of the specific heat capacity of DTPC SUV stored at 4 °C for 3 (A) or 31 days (B) and of DTPC LMV (C). In all cases, cooling scans are shown, although heating scans were quite similar, except for the well-documented hysteresis in the "pretransition" (Lentz et al., 1978).

Just as for DMPC and DPPC SUV, we wished to contrast the phase behavior of DTPC stored above as opposed to below their phase transition. When stored below their phase transition temperature, DTPC SUV developed a pronounced high-temperature peak in their specific heat capacity profile, as shown in Figure 8A. After extensive storage at 4 °C, the heat capacity profile of DTPC SUV (Figure 8B) showed mainly one sharp peak at 27.3 (heating) or 27.8 °C (cooling). The enthalpy under this peak was 5.2 ± 0.5 kcal/mol. The large uncertainty in this value is due to ambiguities in the base line, probably associated with remnants of a small vesicle peak. As with DMPC (Parente & Lentz, 1984), the phase behavior of the fusion product of cold-stored DTPC SUV was distinct from that of DTPC LMV, shown in Figure 8C (peak at 26.6 ± 0.5 °C; enthalpy of 5.94 ± 0.06 kcal/mol).

To determine the kinetics of DTPC SUV size growth above the phase transition, the phase behaviors of samples stored at 41.5 °C for varying lengths of time were recorded in cooling scans. The resolved enthalpies associated with the SUV peak (peak β) and the fusion product peak (peak α) are recorded in Table II. These data were used to calculate the fraction, f_L, of lipid contributing to the fusion product peak in specific heat capacity profiles. These values of f_L are plotted in Figure 9 as a function of storage time and have been analyzed according to the pseudo-first-order reaction scheme given in the Appendix. This analysis yielded an estimate of the rate constant for vesicle size growth (k = 0.0047 ± 0.0008 h^{-1} for f_L^* = 0.21), which is reasonably consistent with that estimated for DMPC at 42 °C (k = 0.013 ± 0.001 h^{-1} for f_L^* = 0.20).

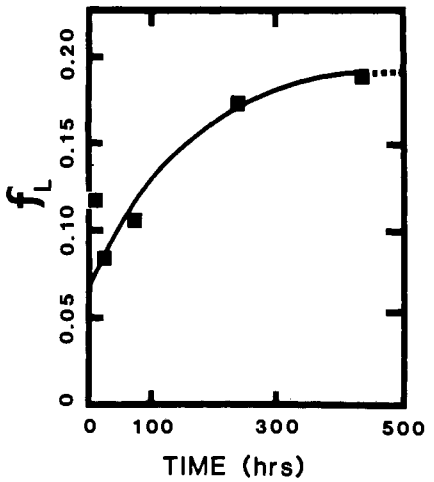

FIGURE 9: Time course for the appearance of a large vesicle contribution to DTPC SUV phase behavior. Data were taken from cooling thermograms of SUV samples (e.g., see Figure 7) stored at 41.5 °C. The fraction of lipid present as large vesicles (f_L) was derived as described in the Appendix, from the resolved peak enthalpies recorded in Table II. A value of 5.9 kcal/mol (LMV and low-temperature fusion product transition enthalpy; see Figure 8B and text) was assigned to ΔH_L for the purpose of calculating f_L, and a value of 0.21 was assigned to the long-time value of f_L (f_L^*).

This qualitative agreement between the results with DMPC and DTPC SUV demonstrates unequivocally that phospholipid hydrolysis was not necessary for the vesicle size growth that we have observed above T_m.

We note that the data of Figure 9 do not pass through $f_L = 0$, as discussed above in relation to Figure 7. In addition, the contribution due to fusion product was anomalously high in the 6-h time point (see Figure 9 and Table II). We have tentatively attributed this to the possible requirement for a longer annealing time for DTPC as opposed to DMPC or DPPC SUV (see above and Table I). Because of this anomalous behavior at short incubation times, the t = 6-h point was ignored in the kinetic analysis, and there was no constraint that the least-squares line pass through zero. Under these conditions, the value chosen for f_L^* (0.21) led to a reasonable estimate for f_L^0 (0.065), consistent with the data in Figure 9. Smaller values of f_L^* led to poor predictions of f_L^0.

Discussion

SUV Phase Behavior. In this study, we have taken advantage of our unique, high-sensitivity, cooling calorimeter to establish the phase behavior of small unilamellar phosphatidylcholine vesicles, free of the complications of large vesicle formation below the phase transition. To our knowledge, only one previous report (Lichtenberg et al., 1984) has accomplished this although another study has come close to this goal by using a low-sensitivity calorimeter, short equilibration times, and rapid scan rates (Gaber & Sheridan, 1982). As for our work, Lichtenberg et al. and Gaber and Sheridan reported a DPPC SUV phase transition having only one peak. However, the details of enthalpy and peak position associated with the phase transition reported by Gaber and Sheridan were suspect due to the inability to allow adequate time for equilibration before and during the scan.

Several features of SUV phase behavior are apparent from our results. First, as previously reported by Lichtenberg et al. (1984), small vesicles display a low-temperature transition that might correspond to the pretransition in LMV. This transition is visible in both cooling (27.4 °C) and heating (27.8 °C) scans in Figure 1. We have estimated the enthalpy of this transition to be 280 cal/mol. These results compare favorably with those reported by Lichtenberg and colleagues (ΔH = 130 cal/mol, T_m = 28.0 °C). The pretransition in the DMPC data is not so clearly defined but apparently corresponds to a low-temperature shoulder (12.6 °C cooling, 14.7 °C heating) on the broad main transition peak. This is the first report of a pretransition in SUV prepared from DMPC.

Second, our work has revealed a significant difficulty in defining the enthalpy associated with the main phase transition in SUV. This is due to the ambiguity in establishing the base line on the low-temperature side of the transition (Figure 1). If we allow for a curved base line (dotted line in Figure 1A), the integrated enthalpy below the main peak is 6.5 kcal/mol, in good agreement with the previous estimates of 6.3 kcal/mol (Suurkuusk et al., 1976), 6 kcal/mol (Gaber & Sheridan, 1982), and 5.5 kcal/mol (Lichtenberg et al., 1984). However, if we include a broad, low-temperature shoulder that clearly deviates from our flat base line, the total enthalpy is 9.3 kcal/mol, roughly what we have found for the main transition of DPPC LMV (8.7 kcal/mol; Parente & Lentz, 1984). The origin of this broad contribution is unclear. However, the ratio of the enthalpies of the sharp and broad contributions is 2.3, roughly the mass ratio (2.1) reported for the outer leaflet relative to the inner leaflet of the DPPC SUV bilayer (Huang, 1969). Aside from accounting for the base-line anomaly in the DPPC SUV scan, the existence of separate inner and outer leaflet peaks could also account for the substantial breadth and complexity of the DMPC SUV heat capacity profile (Figure 1B).

Finally, our ability to define the SUV transition free of contributions from larger vesicles has allowed us to estimate the size of the cooperative unit associated with the main transition, using the method of Mountcastle et al. (1978) to determine the ratio of the van't Hoff to calorimetric enthalpies. For DPPC SUV, we found this to be 16 (using ΔH^{cal} = 9.3 kcal/mol) or 31 (with ΔH^{cal} = 6.5 kcal/mol). We can make a more detailed interpretation in terms of the cooperative unit associated with the independent melting of the outer or inner (see discussion in the preceding paragraph) monolayers. In this interpretation, the poorly packed acyl chains of the inner monolayer (Wu et al., 1985) melt with very low cooperativity (cooperative unit = 19) compared to the more efficiently packed outer monolayer (cooperative unit = 31). These cooperative unit values compare to 23, 200, and 261 for DPPC dialyzed octyl glucoside vesicles, fusion vesicles, and LMV, respectively (Parente & Lentz, 1984). For DMPC SUV, our results yielded a cooperative unit size of 15, which compares with 60 and 254 for dialyzed octyl glucoside vesicles and LMV, respectively (Parente & Lentz, 1984). These results contrast with a previous report (Gruenewald et al., 1979) that vesicle curvature had little or no effect on the cooperative unit of DMPC vesicles, estimated to be 100–150 for all vesicles having radii between 200 and 400 Å. It should be noted that the ethanol-injection vesicles prepared by Grueneweld et al. were all of intermediate curvature and did not span the range of highly curved to essentially uncurved membranes, as did our preparations (Parente & Lentz, 1984; this work).

SUV Fusion above the Order–Disorder Phase Transition. The instability of SUV below their phase transition has been widely reported and studied [e.g., see Suurkuusk et al. (1976), Larrabee (1979), Schullery et al. (1980), Sornette et al. (1981), Wong et al. (1982), and McConnell and Schullery (1985)]. It has been assumed universally that the increase in vesicle size associated with this instability resulted from a fusion process. However, there has been no clear demonstration of this, at least in terms of the generally accepted

operational definition of fusion: trapped contents mixing, bilayer components mixing, limited leakage.

Just as SUV are believed to fuse below their phase transition, it has been widely reported by the same researchers that SUV preparations are stable when stored above their phase transition. However, if one carefully examines the *data* (as opposed to the conclusions) from the above-referenced papers, it would seem that some larger vesicle species may form slowly and to a small extent in SUV preparations even above the main phase transition [e.g., see Figure 7 of Suurkuusk et al. (1976), Figure 6 of Larrabee (1979), Figure 1 of Schullery et al. (1980), and Figure 2 of Sornette et al. (1981)]. Our high-sensitivity cooling calorimeter has allowed us to quantitate this vesicle size increase unambiguously.

Just as others have explained SUV instability below the phase transition, we assume that the observed vesicle size increase above T_m is due to fusion. However, the slow rate of this process has made it impossible to test this assumption by standard contents mixing, lipid mixing, or contents leakage assays. We note that one paper has reported evidence for the mixing of internal contents of DPPC SUV at 48 °C (Taupin & McConnell, 1972). However, this evidence was clouded by the rate of vesicle contents leakage, as would be any attempt on our part to demonstrate fusion by contents mixing. Despite the problems with conclusively demonstrating fusion, it is difficult to envision another mechanism to explain the observed size growth. Net lipid transfer from small to large vesicles is unlikely, since this cannot explain the total disappearance of a small vesicle, and small vesicles must disappear to explain the results in Figure 5. Vesicle rupture and resealing could account for our results, but without the presence of a fusogen or other perturbant, it is hard to imagine what would drive such a process. For lack of a more plausible mechanism, we assume that vesicle size growth is due to fusion of colliding vesicles whose bilayers are unstable due to their high radius of curvature. Presumably, this process should stop once the stress of high membrane curvature is relieved. From our phase behavior, freeze–fracture electron microscopy, and trapping results, it appears that the products of SUV fusion above the phase transition are intermediate-sized vesicles of reduced but not negligible curvature. The phase behavior of these vesicles is distinct from that of the large unilamellar vesicles formed upon storage below the phase transition.

It may be that the relatively small shift in vesicle size distribution that we have observed (see Figure 5) has made detection of SUV instability above the phase transition difficult. For instance, one study that has carefully examined the issue of SUV stability above T_m has concluded that fusion did not occur until several degrees below the phase transition (McConnell & Schullery, 1985). These authors used size-exclusion chromatography to characterize unfractionated DPPC SUV preparations stored under different conditions. Such unfractionated preparations are expected to contain a substantial number of intermediate-sized vesicles (300–500-Å diameter), in contrast to the fractionated population that we have studied. It is unlikely that size-exclusion chromatography could have detected a small increase in the fraction of lipid incorporated into intermediate-sized vesicles in such unfractionated preparations. Our use of freshly fractionated preparations as well as the documented extreme sensitivity of membrane phase behavior to vesicle size, especially in the small to intermediate size range (Lichtenberg et al., 1981), has made it possible for us to detect the instability that we report.

Kinetics of Fusion above the Phase Transition. By recording the enthalpy of the order–disorder phase transition associated with the high-temperature SUV fusion product, we have been able to estimate the pseudo-first-order rate constants for the fusion process. Two points should be made in discussing these data. First, we do not expect the kinetic mechanism for the fusion process to be true first order. However, our data were treated according to a pseudo-first-order model, since it was not our purpose to examine the concentration dependence of the process. For this reason, all studies were carried out at a phospholipid concentration of 5.5 ± 0.2 mM. If the process is second order, the second-order rate constants could be obtained by dividing the pseudo-first-order constants by this concentration. Second, it is unlikely that the fusion reported here reflects solely the hydrolytic degeneration of phospholipid due to storage at high temperatures. We did not detect degradation products for up to 12–15 days of storage, and, even when detected, these were not present in major amounts. In addition, the results obtained at 41.5 °C with DTPC were quite similar to those obtained with DMPC at 42 °C. DTPC, being an ether lipid, is not nearly as sensitive to hydrolysis as is DMPC, an ester lipid.

With these points in mind, the kinetic analysis of our data demonstrates, first, that small vesicle preparations should be used within a few hours of size fractionation. Second, the substantial increase in fusion rate with temperature (see Figure 6) indicates a large activation energy for the rate-limiting step of the process. From our data, we estimate this to be 30–40 kcal/mol. The large magnitude of this activation energy suggests that close juxtaposition of vesicle bilayers (Parsegian & Rand, 1983) may be the rate-determining step for spontaneous fusion of SUV. Third, it is also clear from our data (see Figure 6) that the extent of DMPC SUV fusion increased with temperature. This probably reflects an increased probability of vesicle–vesicle collisions at higher temperature. From a practical point of view, this means that when storage is necessary, SUV should be stored just above their phase transition. Finally, we note that only the smallest, most highly curved vesicles fused to form intermediate-sized vesicles. The intermediate-sized vesicles appear to be stable above their phase transition, although our data do not rule out the possibility that these, too, fuse, but at a much slower rate than do the highly curved species.

ACKNOWLEDGMENTS

We thank Dr. Roberta Parente for advice and several helpful discussions related to this work and for reading and criticizing the manuscript. Thanks are also extended to Susan Windes for help with Figure 5, to Pamela Wall for help with the trapped volume experiments, and to D. Massenburg and S. Burgess for criticizing the manuscript.

APPENDIX

Two-State, Pseudo-First-Order Analysis of Enthalpy Data. Suurkuusk et al. (1976) assumed a two-state equilibrium to exist between small (S) and large (L) vesicles (eq A1).

$$S \underset{k_-}{\overset{k_+}{\rightleftharpoons}} L \qquad \text{(A1)}$$

Because the spontaneous reversal of large vesicle formation has never been demonstrated, we must modify this treatment to account for an irreversible process (eq A1a).

$$S \xrightarrow{K} L \qquad \text{(A1a)}$$

The following relationships were assumed to exist between the phase transition enthalpies per mole of lipid incorporated into small and large vesicles (ΔH_S and ΔH_L), the mole fraction

of lipid existing at any time in small and large vesicles (f_S and f_L), and the enthalpy per total mole of lipid under peaks β and α (ΔH_β and ΔH_α; see Table I):

$$\Delta H_L = \Delta H_\alpha / f_L$$
$$\Delta H_S = \Delta H_\beta / f_S \quad \text{(A2)}$$
$$1 = f_L + f_S$$

The fraction of lipid in large vesicles was observed to approach a limiting value of f_L^*. This fraction must be estimated directly from the data. The fact that not all the enthalpy of melting is shifted from the small vesicle to the intermediate-sized vesicle peak (i.e., $f_L^* \neq 1$) indicates that not all SUV can convert to intermediate-sized vesicles. We may apply our treatment only to that fraction of SUV that can undergo reaction A1a. From these assumptions, the following kinetic expression can be written:

$$(1 - f_L')/(1 - f_L'^0) = \exp(-kt) \quad \text{(A3)}$$

where the quantities f_L' and $f_L'^0$ are calculated as f_L/f_L^* and f_L^0/f_L^*, respectively, where f_L^0 is the fraction of intermediate-sized vesicles at zero time.

Registry No. DPPC, 63-89-8; DMPC, 18194-24-6; DTPC, 36314-48-4.

References

Barenholz, Y., Gibbs, D., Litman, B. J., Goll, J., Thompson, T. E., & Carlson, F. D. (1977) *Biochemistry 16*, 2806–2810.

Bligh, E. G., & Dyer, W. J. (1959) *Can. J. Biochem. Physiol. 37*, 911–917.

Bramhall, J. (1986) *Biochemistry 25*, 3479–3486.

Chen, P. J., Jr., Torribara, T. Y., & Warner, H. (1956) *Anal. Chem. 28*, 1756–1758.

Dufour, J. P., Nunnally, R., Buhla, L., Jr., & Tsong, T. Y. (1981) *Biochemistry 20*, 5576–5586.

Gaber, B. P., & Sheridan, J. P. (1982) *Biochim. Biophys. Acta 685*, 87–93.

Gruenewald, B., Stankowski, S., & Blume, A. (1979) *FEBS Lett. 102*, 227–229.

Gruner, S. M. (1985) *Proc. Natl. Acad. Sci. U.S.A. 82*, 3665–3669.

Huang, C. (1969) *Biochemistry 8*, 344–352.

Huang, C., & Mason, J. T. (1978) *Proc. Natl. Acad. Sci. U.S.A. 75*, 308–310.

Larrabee, A. L. (1979) *Biochemistry 18*, 3321–3326.

Lawaczeck, R., Kainosho, M., & Chan, S. I. (1976) *Biochim. Biophys. Acta 443*, 313–330.

Lentz, B. R., Barenholz, Y., & Thompson, T. E. (1976) *Biochemistry 15*, 4529–4537.

Lentz, B. R., Freire, E., & Biltonen, R. L. (1978) *Biochemistry 17*, 4475–4480.

Lentz, B. R., Hoechli, M., & Barenholz, Y. (1981) *Biochemistry 20*, 6803–6809.

Lentz, B. R., Alford, D. R., Jones, M. E., & Dombrose, F. A. (1985) *Biochemistry 24*, 6997–7005.

Lichtenberg, D., Freire, E., Schmidt, C. F., Barenholz, Y., Felgner, P. L., & Thompson, T. E. (1981) *Biochemistry 20*, 3462–3467.

Lichtenberg, D., Menashe, M., Donaldson, S., & Biltonen, R. L. (1984) *Lipids 19*, 395–400.

McConnell, D. S., & Schullery, S. E. (1985) *Biochim. Biophys. Acta 818*, 13–22.

Mountcastle, D. B., Biltomen, R. L., & Halsey, M. J. (1978) *Proc. Natl. Acad. Sci. U.S.A. 75*, 4906–4910.

Parente, R. A., & Lentz, B. R. (1984) *Biochemistry 23*, 2353–2362.

Parsegian, V. A., & Rand, R. P. (1983) *Ann. N.Y. Acad. Sci. 416*, 1–12.

Roseman, M. A., Lentz, B. R., Sears, B., Gibbs, D., & Thompson, T. E. (1978) *Chem. Phys. Lipids 21*, 205–222.

Sackmann, E., Kotulla, R., & Heiszler, F. J. (1984) *Can. J. Biochem. Cell Biol. 12*, 778–788.

Schullery, S. E., Schmidt, C. F., Felgner, P., Tillack, T. W., & Thompson, T. E. (1980) *Biochemistry 19*, 3919–3923.

Sheetz, M. P., & Chan, S. I. (1972) *Biochemistry 11*, 4573–4581.

Sornette, D., Hesse-Bezot, C., & Ostrowsky, N. (1981) *Biochimie 63*, 955–959.

Suurkuusk, J., Lentz, B. R., Barenholz, Y., Biltonen, R. L., & Thompson, T. E. (1976) *Biochemistry 15*, 1393–1401.

Taupin, C., & McConnell, H. M. (1972) in *Mitochondria Biomembranes*, pp 219–229, North-Holland, Amsterdam.

Thompson, T. E., Huang, C., & Litman, B. J. (1974) in *The Cell Surface in Development* (Moscona, A. A., Ed.) pp 1–16, Wiley, New York.

Wong, M., Anthony, F. H., Tillack, T. W., & Thompson, T. E. (1982) *Biochemistry 21*, 4126–4132.

Wu, W.-G., Dowd, S. R., Simplaceanu, V., Peng, Z.-Y., & Ho, C. (1985) *Biochemistry 24*, 7153–7161.